**PAPER** • **OPEN ACCESS**

# Performance assessment of a heat and moisture dynamic simulation model in IDA ICE by the comparison with WUFI Plus

To cite this article: F Frasca *et al* 2018 *IOP Conf. Ser.: Mater. Sci. Eng.* **364** 012024

IOP Conf. Series: Materials Science and Engineering **364** (2018) 012024 doi:10.1088/1757-899X/364/1/012024

# Performance assessment of a heat and moisture dynamic simulation model in IDA ICE by the comparison with WUFI Plus

**F Frasca[1*], C Cornaro[2] and AM Siani[3]**

[1] Sapienza Università di Roma, Department of Earth Sciences, P.le A. Moro 2, 00185 Rome, Italy.
[2] Università degli Studi di Roma "Tor Vergata", Department of Enterprise Engineering, Via del Politecnico 1, 00133 Rome, Italy
[3] Sapienza Università di Roma, Department of Physics, P.le A. Moro 2, 00185 Rome, Italy.

* Corrisponding author: f.frasca@uniroma1.it

**Abstract**. Recently, in the field of preventive conservation, the use of accurate whole-building dynamic simulation models is becoming an effective approach for preventing degradation phenomena due to changes in indoor historic climate. Among microclimate parameters, the moisture plays a key role in the degradation of organic-hygroscopic artworks as well as in the durability of building components. Some simulation codes combine both heat and moisture transfer calculations, however their capability to accurately model the moisture transport is limited. The HMWall model coupled with IDA Indoor Climate and Energy (IDA ICE) software is one of those models.
This study aims at comparing the performance of the HMWall model with respect to WUFI Plus, developed by Fraunhofer Institute for Building Physics (IBP). Temperature (T) and relative humidity (RH) provided by both codes in the case of a building envelope with no infiltration, windows and incoming solar radiation, are compared. This allows to assess whether both models calculate the moisture transport throughout walls in the same way. *Dynamic simulations have been run over a year by using different T-RH outdoor conditions.* Even if both models are based on the same heat and moisture transport equations, RH behaviour simulated by HMWall is significantly different from that by WUFI Plus. This mainly depends on the calculation of saturated vapour pressure ($p_{sat}$) inside the material. Then, the Common Exercise 3 has been applied to test if HMWall were capable to affect indoor RH when cladding materials with different sorption behaviour are used.
The new HMWall implemented model is resulted more effective than the previous one, and in the case of simplified building, RHs modelled by both programs are highly correlated.

## 1. Introduction

In the last years, a commensurable interest on the use of accurate whole-building dynamic simulation models has been shown in preventive conservation studies, even though up to now this modelling approach has been extensively applied to determine energy efficiency of buildings [1-3] and thermal comfort optimization [4]. At the present time, the whole-building dynamic simulation model is also becoming an effective methodology to assess the microclimate risk on artworks when changes in indoor historic climate occur due to refurbishment or climate change [5]. Physical measurements and simulation provide a complete evaluation of the indoor climate and interactions among object-environment and building-environment.

Both temperature (T) and relative humidity (RH) can induce degradation phenomena [6]. Specifically, RH is the main responsible of the deterioration in organic-hygroscopic artworks as well as in the durability of building components. For this reason, an accurate simulation and control of RH behaviour in these sites is of significant importance.

Most of simulation codes has been developed to model moisture exchanges between indoor and outdoor environments setting a specific moisture storage capacity to the interior of the building [7] and not to model the moisture flow between the air and porous surfaces, such as walls [8]. Some of them use two simulations distinctly but running together: one for building energy or envelope simulation and one for modelling the heat and moisture transport between the air and porous surfaces. The HMWall model coupled with IDA Indoor Climate and Energy (IDA ICE) and WUFI® Plus (hereafter called WUFI) belong to the latter group [9], and their performance will be compared in this paper.

*WUFI® Plus is a holistic model based on the hygrothermal envelope calculation model developed by H.M. Kunzel's at Fraunhofer Institute for Building Physics (IBP) [10]. It takes into account sources and sinks of moisture inside a component, liquid water transport, diffusion and vapour ab - and de-sorption as well as the thermal parameters [11].Field and laboratory validation are performed for WUFI® Plus more than for other hygrothermal simulation tools [12]. Moreover, it has been widely compared with other hygrothermal software [13-15] and used within the European project Climate for Culture (CfC) [16].*

*The HMWall model coupled with IDA ICE has been developed in 1999 [17] and, then, updated in 2011. In the first version, the moisture transfer was modelled by one moisture-transfer potential (the humidity by volume), whereas the liquid water transport and the hysteresis of moisture transport were not taken into account. This version, coupled with IDA ICE 3.0, was used within the IEA Annex 41 [18] and to model the hygrothermal behaviour inside historical buildings [19-20]. In 2011, the code has been edited according to the same balance heat and moisture equations of WUFI [10] (section 1.1), mainly due to the lack of the hygrometric data of materials required to run the code. The latter has been validated to conform with the EN 15026:2007 standard validation test; however, no study about this HMWall model has been published yet.*

*Currently, the HMWall code differs from WUFI for the following features: the percentage of material porosity is not taken into account and hygrometric properties of materials, not available in the software library, have to be extracted from available database and time-by-time compiled in the model object. Hygrothermal curves can only be derived by mathematical relations and not built by using experimental data. Finally, heat or moisture sources (e.g. fraction of driving rain, pipe failures, etc.) cannot be added by the users within the wall component.*

This paper aims at investigating for the first time the capability of the HMWall model, updated in 2011 and coupled with IDA ICE 4.7.1 released in 2015, to calculate the moisture transport across walls at increasing complexity of the building structures and boundary conditions. First, a simplified building envelope was modelled in IDA ICE and WUFI and, then, a comparison of time series of RH modelled by both models, was carried out. This has allowed to assess only the moisture transfer across walls, which is the main focus of this exercise. Then, the Common Exercise 3 (CE3) developed by the Fraunhofer IBP in the framework of IEA Annex 41 and also used within the CfC was applied to evaluate the capability of HMWall to simulate the influence of different cladding material in the rooms on the RH.

A successful performance of HMWall model coupled with IDA ICE will provide a validated improvement of IDA ICE packages to both users and experts of preventive conservation of historical buildings and artworks.

### *1.1. Basic governing equations*

Both models are based on the following balance equations for heat (eq. 1) and moisture (eq. 2) transfers [10]:

$$\frac{dH}{dT}\cdot\frac{\delta T}{\delta t}=\nabla\cdot\left(\lambda\cdot\nabla\vartheta\right)-h_v\cdot\nabla g_v \qquad 1)$$

where *dH/dT* is the heat capacity of the wet material (J/m$^3$·K); *δT/δt* is the change of temperature (T) in time (K/s),; $\lambda$ is the thermal conductivity of the wet material (W/m·K); $h_v\cdot\nabla g_v$ is the latent heat source, $h_v$ is the evaporation enthalpy of water (J/kg) and $g_v$ is the vapour diffusion flux (kg/m$^2$·s).

$$\frac{dw}{d\varphi}\cdot\frac{\delta\varphi}{\delta t}=\nabla\cdot\left(g_w+g_v\right) \qquad 2)$$

where *w* is the equilibrium water content (w) and $\varphi$ is the relative humidity*; dw/dφ* is the moisture storage capacity of the material (kg/m$^3$); *δφ/δt* is the change of relative humidity (φ or RH) in time (1/s); $g_w$ is the capillary moisture flux (kg/m$^2$·s), i.e. $D\varphi\cdot\nabla\varphi$ with $D\varphi$ as the liquid conduction coefficient of water (kg·m/s); $g_v$ as above, i.e. $\delta_p\cdot\nabla(RH\cdot p_{sat})$ with $\delta_p$ as the water vapour permeability of material (kg/m·s·Pa) and $p_{sat}$ as the saturated vapour pressure of water (Pa).
In both codes, $\delta_p$ is calculated as the ratio between $\delta_a$ (the water vapour permeability of air given by Schirmer's equation) and $\mu$ (the dimensionless vapour resistance factor of the material).
Concerning *Dφ,* the codes use two different equations both reported in [10]. In WUFI, *Dφ* is the product between the capillary transport coefficient (*Dw*), once the water absorption coefficient of the material ($A_w$) is known, and *dw/dRH.* In HMWall, *Dφ* is calculated taking into account both wet ($\mu_w$) and dry ($\mu_d$) cup vapour diffusion resistance factor. One of the main issues is that $\mu_w$ is not available in database and, if any, only for few materials.
The sorption curves are calculating as a function of RH and not dependent on T, since the equilibrium water content (w) is assumed to be little sensitive to T changes [10].
Equations 1) and 2) are strongly related when the number of variables in both equations are limited to T and RH. In fact, it follows that: λ in eq.1 is moisture-dependent; the enthalpy flux is related to $g_v$ so that heat transfer considers the contribution of water vapour phase change; and $g_v$ is dependent on T through $p_{sat}$.

## 2. Material and method

In this paper, the examination of the performance of the HMWall model coupled with IDA ICE 4.7.1 has been carried out as shown in the schematic workflow in Figure 1. The workflow consists of test cases at increasing complexity of the building envelope. In this way, it has been possible to assess: a) the capability of HMWall to calculate the heat and moisture transport across walls when the only difference between indoor and outdoor climate is given by RH (first test case); b) *the capability of HMWall to simulate the influence of different cladding material on the indoor RH (second test case). All simulations have been run in transient conditions using hourly step over a year.*

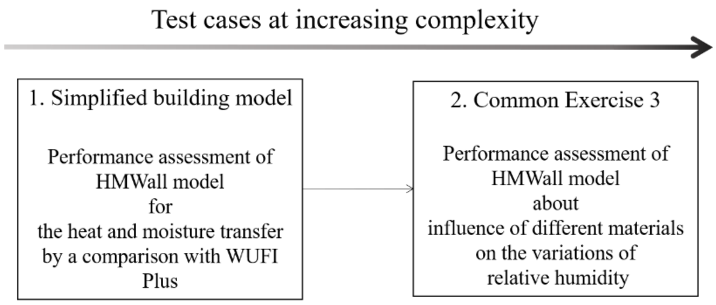


**Figure 1.** Schematic workflow of methodology applied in this study.

### *2.1. A simplified building model*

The first test case is to perform the simulation considering a simplified building having the following characteristics: an envelope of a parallelepiped with a volume of 26.0 m$^3$, with height of 2.6 m and a length of 2.5 m oriented in east-west direction and of 4.0 m in north-south. It was designed without windows and with a flat ceiling. All opaque components are built by a monolayer of lime silica brick of 0.2 m, whose hygrothermal properties are reported in Table 1. Air changes by infiltration are set to 0.0 $h^{-1}$ and no thermal bridges are taken into account. The initial values of indoor T and RH are 10°C and 50%, respectively. *The file of the external environmental conditions consists of T and RH values taken at 1-hour time slot, so that no contribution from solar radiation and ventilation can affect the heat and moisture transfer calculations. This is very important to avoid misleading with input parameters, such as wind, infiltration or radiation, whose setting varies from a code to another code. Two simulations are run with outdoor temperature $T_{out}$=10°C and relative humidity $RH_{out}$=60% (the first simulation) and $T_{out}$=10°C and $RH_{out}$=40% (the second simulation). A third simulation is run setting $T_{out}$=10°C and $RH_{out}$ as a sinusoidal curve ($RH_{min}$=42.0% and $RH_{max}$=58.0%), in order to assess the response of both models when there is a seasonal variation of RH over a year. The simulations are performed over the period from January, 1st to December 31st at 1-hour step.* In this test case, variations of RH are mainly driven by water vapour partial pressure ($p_v$) transferred across walls and by the moisture storage capacity of envelope, since the heat transfer is constant and, consequently, the $p_{sat}$ which is a function of T is constant.

**Table 1**. Hygrothermal properties of lime silica brick as provided by *MASEA Datenbank - Materialdatensammlung für die energetische Altbausanierung*

| Hygrothermal properties | Value |
|---|---|
| Density (ρ) | 1830.0 kg/m$^3$ |
| Heat capacity ($c_p$) | 850.0 J/(kg·K) |
| Thermal conductivity (λ) | 1.0 W/(m·K) |
| Wet cup vapour diffusion resistance factor ($\mu_w$) | 18.0 |
| Dry cup vapour diffusion resistance factor ($\mu_d$) | 27.0 |
| Free water saturation ($W_f$) | 257.1 kg/m$^3$ |
| Equilibrium water content at 80% rel hum ($W_{80}$) | 27.5 kg/m$^3$ |
| Water absorption coefficient ($A_w$) | 0.059 kg/(m$^2$·s$^{1/2}$) |

### *2.2. The Common Exercise 3 (CE3)*

The Common Exercise 3 (CE3) consists of a double climatic chamber (test room and reference room) [7]. A detailed description of this exercise can be found in [18]. The CE3 aims at simulating the indoor climate of two rooms in order to assess the influence of the sorption of different material on the RH in the rooms. *Four boundary conditions around the rooms are set, so that internal walls are surrounded by controlled T and RH areas, whereas external walls are exposed to weather data of Holzkirchen, i.e. its TRY (Test Reference Year-type) weather data*. Indoor T is controlled by a small radiator (with maximum heat dissipation of 1000 W) at 20±2°C and the moisture production corresponds to 2.4 kg/day. Natural air changes by infiltration correspond to 0.09 $h^{-1}$ for the reference room and 0.07 $h^{-1}$ for the test room, whereas mechanical ventilations are 0.63 $h^{-1}$ and 0.66 $h^{-1}$, respectively. The exercise consists in 3 steps, in which simulations are run with different cladding materials in the test room: 1) test room only with aluminium foil; 2) test room with gypsum boards on the walls and 3) test room with gypsum boards on the walls and roof. This paper will show the results from HMWall coupled with IDA ICE 4.7.1, to assess the influence of different materials on RH peaks [18], in the case of test room.

## 3. Results and discussion

### *3.1. A simplified building model*

Figure 2 shows the scatter diagram (HMWall *vs* WUFI Plus) of indoor modelled RH values driven only by the moisture transport across walls. The initial indoor RH is 50% and the boundary RH is 60%. The WUFI RHs tend to increase towards the RH boundary value, whereas the HMWall RHs remain quite constant around initial condition ($RH_{max}$=50.3%). The slope of linear regression (red line in Figure 1) is 0.03%, demonstrating that the two codes have modelled indoor RH with significant differences. In fact, the RHs modelled by HMWall seem not be affected by the moisture transport across walls, suggesting that no difference between indoor and boundaries RH has been detected.

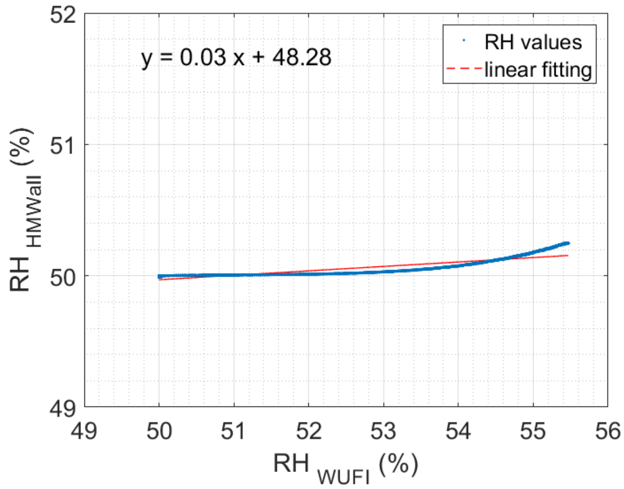


**Figure 2.** Scatter diagram of simulated RH values (HMWall *vs* WUFI Plus) over a year. The hygrometric boundary condition is set to 60%. Temperature is 10°C, constant inside and outside the envelope.

Since T was constant ($T_{in}$ = $T_{out}$ = 10°C), the $p_{sat}$ was expected to be constant and equals to 12.30 hPa according to Magnus formula [21] for the pressure of water vapour at the saturation. It was observed that the $p_{sat}$ calculated by HMWall was 13.08 hPa.

Moreover, it was found that the codes used a different calculation of the water vapour transfer ($g_v$) between the wall surface and the boundary air layer close to it. In WUFI Plus, $g_v$ is determined in analogy to that used for the heat transfer, and water vapour transfer coefficient ($\beta_p$) is derived from the convective heat transfer coefficient. In HMWall, the calculation of moisture transfer at the boundaries of the building component is different from that in WUFI, since $g_v$ is calculated as the discretized derivative of the vapour pressure between the last layer of wall material and the boundary air layer.

For the above reasons, we have modified this HMWall model (hereafter called HMWall_old) and in order to verify the sensibility of the code at $g_v$ calculated as described by [10] and used in the WUFI Plus, two HMWall codes have been implemented as follows:

- HMWall (A), where only $p_{sat}$ has been updated;
- HMWall (B), where $p_{sat}$ is the same of HMWall (A) and $g_v$ is also calculated as in the same as that in WUFI.

Figure 3 shows the scatter diagrams of the modelled RH values when the boundary conditions are set to $RH_{out}$=60%. RHs modelled by HMWall (A) and HMWall (B) tend to increase over time towards the equilibrium with the boundary condition in accordance with WUFI. Both HMWall (A) and (B) codes underestimate the maximum RH value modelled by WUFI, as if they buffer the moisture transport towards indoor over time. However, the coefficient of determination ($R^2$) is 0.994 for HMWall (A) and 0.996 for HMWall (B) (Table 2), showing a visible improvement of both codes with respect to the HMWall_old ($R^2$=0.771).

When the boundary conditions are drier ($RH_{out}$=40%) than the indoor climate (Figure 4), RHs modelled by HMWall (A) and HMWall (B) tend to decrease in accordance with WUFI. However, HMWall (A) (left panel in Figure 4) shows a better behaviour with respect to HMWall (B) with a slope of linear fitting close to unity. HMWall (B) (right panel of Figure 4) seems to go in equilibrium with boundaries more rapidly than the other two. The $R^2$ (Table 2) is 0.998 for HMWall (A) and 0.993 for HMWall (B).

Figure 5 shows the scatter diagrams of the modelled RH values when the hygrometric boundary conditions are defined as a sinusoidal curve. RH values modelled by both HMWall (A) and HMWall (B) are highly correlated with those modelled by WUFI. The slope of both linear fittings is 0.78, showing that both HMWall codes are in accordance to each other, when the hygrometric boundary conditions are more complex than the previous cases whose boundary conditions are constant.

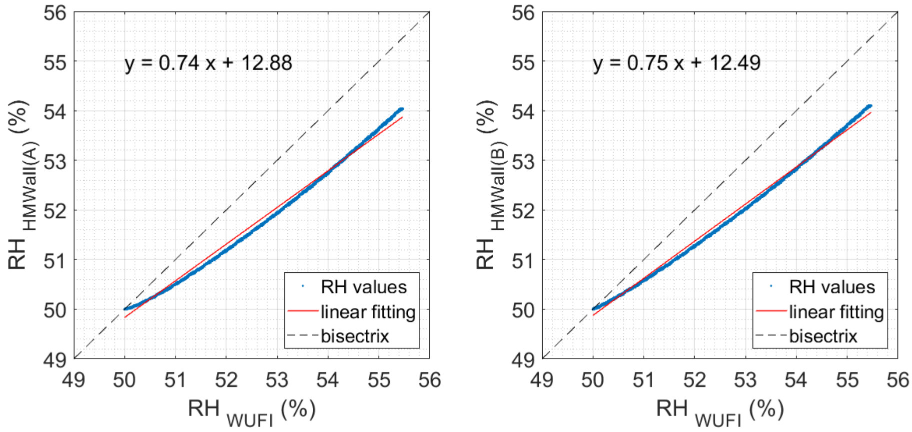


**Figure 3.** Scatter diagram of modelled RH values (HMWall *vs* WUFI Plus) over a year. The hygrometric boundary condition is set to 60%. T was constant ($T_{in} = T_{out} = 10°C$).

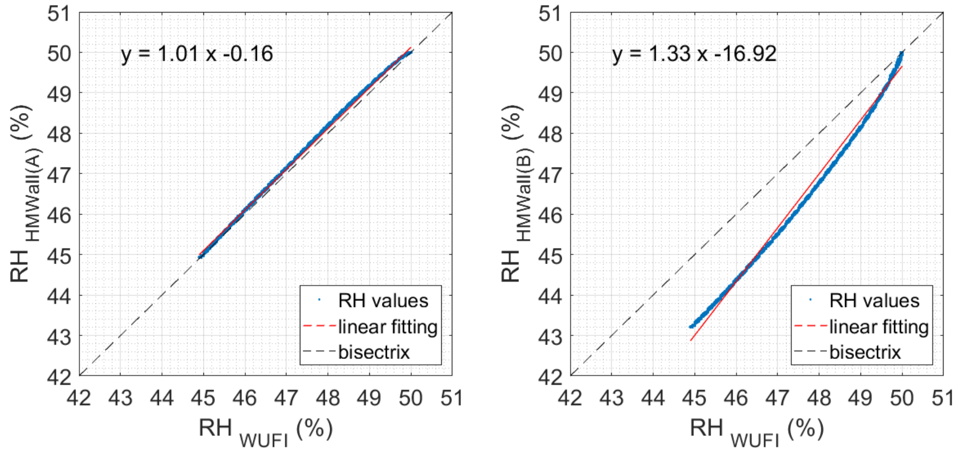


**Figure 4.** Scatter diagram of modelled RH values (HMWall *vs* WUFI Plus) over a year. The hygrometric boundary condition is set to 40%. T was constant ($T_{in} = T_{out} = 10°C$).

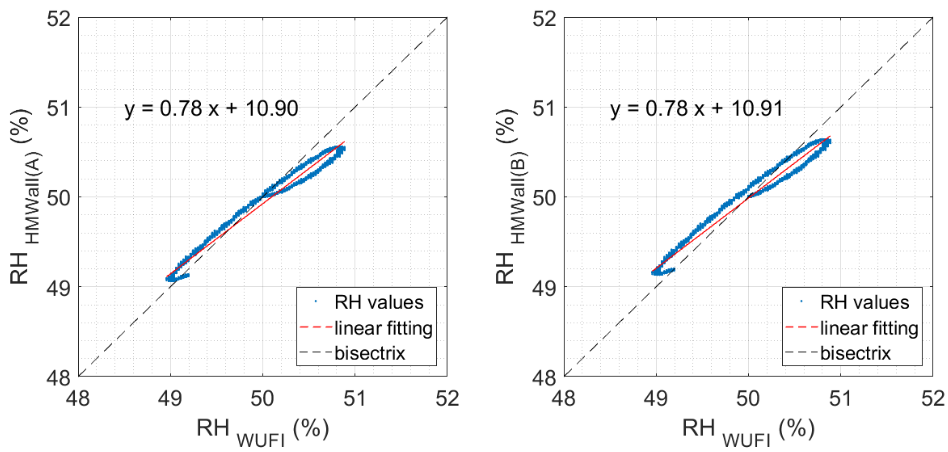


**Figure 5.** Scatter diagram of modelled RH values (HMWall *vs* WUFI Plus) over a year. The hygrometric boundary condition is a sinusoidal curve with a RH decrease in summer. T was constant ($T_{in} = T_{out} = 10°C$).

Table 2 summarizes the $R^2$, MBE (Mean Biased Error) and RMSE (Root Mean Squared Error) calculated for each case. Differences between HMWall (A) and HMWall (B) are at the third decimal place, demonstrating that both codes calculate the moisture transport in similar way. Especially, the HMWall (A) seems to be more in accordance with WUFI when boundaries are drier than indoors, since both the MBE and the RMSE are close to zero. Concerning the HMWall (B), it usually underestimates the RH modelled by WUFI except for the case 3 (MBE = 0.0%). For both the HMWall (A) and (B), the RMSE is close to the unity in the case 1 and close to zero in the case 3, whereas a significant difference is in the case 2 when RMSE is 0.1% and 1.2%, respectively.

**Table 2.** The coefficient of determination ($R^2$), the mean biased error (MBE) and the root mean squared error (RMSE) calculated for HMWall (A) and HMWall (B) in three different hygrometric boundary conditions.

| Parameter | Case 1 | | Case 2 | | Case 3 | |
|---|---|---|---|---|---|---|
| | A | B | A | B | A | B |
| $R^2$ (%) | 0.994 | 0.996 | 0.998 | 0.993 | 0.979 | 0.977 |
| MBE (%) | -0.8 | -0.8 | 0.1 | -1.1 | -0.1 | 0.0 |
| RMSE (%) | 1.0 | 0.9 | 0.1 | 1.2 | 0.2 | 0.2 |

### *3.2. The Common Exercise 3*

Three simulations have been run according to the three steps defined in the common exercise: 1) test room only with aluminium foil; 2) test room with gypsum boards on the walls and 3) test room with gypsum boards on the walls and roof. For this exercise, the maximum daily variations of RH modelled by HMWall (A) and HMWall (B) have been calculated in order to assess the influence of different cladding materials on the indoor RH.

Figure 6 shows that the HMWall (B) generally model higher daily span of RH values with respect to HMWall (A) in both rooms, which result to be very similar each other even though walls and ceiling of the test room were coated by aluminium foils, which means no sorption.

Scatter diagrams of the maximum daily RH variations computed for test2 are in Figure 7. In test room (right panel), the daily RH variations modelled by HMWall (A) are affected by gypsum boards covering walls provoking their reduction up to 6% with respect to HMWall (B). Results from test3 are not shown since no significant differences have been detected with respect to test2.

Generally, the maximum daily variations of RH modelled by HMWall (A) are lower than those modelled by HMWall (B).

## 4. Conclusion

A preliminary comparison between the HMWall model and WUFI Plus has been carried out in the test case of a simplified building. The difference between the two codes mainly depended on the calculation of saturated vapour pressure ($p_{sat}$) inside the layer material. This bug has been found and solved thank to the accessibility and adjustability of the HMWall code by the users. Moreover, it has been found that HMWall model did not calculate the water vapour transfer ($g_v$) between the wall surface and the boundary air layer close to it considering the effect of convection. For this reason, two HMWall codes, called HMWall (A) and HMWall (B), have been derived in order to verify the sensibility of the code at $g_v$ calculated as that in WUFI. Both HMWall (A) and (B) show a visible improvement with respect to the previous HMWall code when $RH_{out}$=60%. The HMWall (A) seems more compatible with WUFI, especially when the hygrometric boundary condition is drier than indoor. In the case of a sinusoidal RH behaviour of boundaries, both HMWall (A) and (B) are quite similar with WUFI.

The main difference between codes can be related to the calculation of the liquid conduction coefficient of water ($D\varphi$). In HMWall, $D\varphi$ only varies as function of the saturated pressure ($p_{sat}$) and the water vapour permeability of material ($\delta_p$), since $\mu_w$ and $\mu_d$ do not change over the calculation, whereas, in WUFI, $D\varphi$ varies according to the water content (w) and hence with RH inside the material.

From the Common Exercise 3, a comparison between HMWall (A) and (B) has been carried out. For both HMWall models, aluminium foils seem not to affect the indoor RH, whereas gypsum boards tend to reduce the maximum daily variations of RHs. However, the effect of gypsum boards is more effective in HMWall (A), suggesting that this model would allow a better simulation of sorption given by gypsum.

Further studies will be addressed in order to compare the results, modelled by modified HMWall models, with respect to the measured indoor data (not available at current state). The future goal is to validate the HMWall model coupled with IDA ICE, that better simulates indoor climate, in order to be definitively implemented in the software.

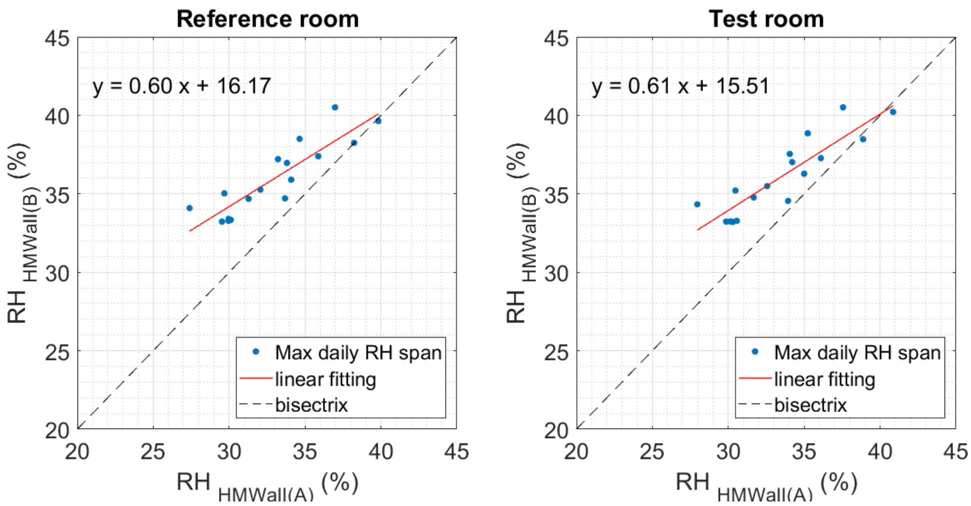


**Figure 6.** Scatter diagram HMWall (B) *vs* HMWall (A) of maximum daily RH variations modelled in reference room (left panel) and test room (right panel) when walls and ceiling are covered only with aluminium foil (test1). Simulation has been run from January 17th to February 2nd 2005.

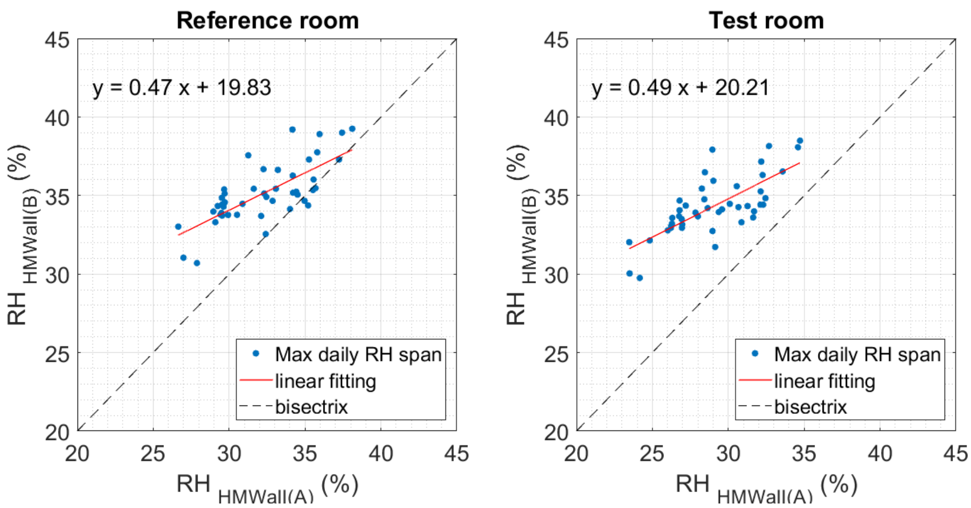


**Figure 7.** Scatter diagram HMWall (B) *vs* HMWall (A) of maximum daily RH variations modelled in reference room (left panel) and test room (right panel) when walls and ceiling are covered with gypsum boards (test2). Simulation has been run from February 14th to March 30th 2005.

**Acknowledgements**

Ph.D. student Francesca Frasca thanks Dr. Florian Antretter, Chief Group of Hygrothermic Department of Fraunhofer Institute for Building Physics (IBP), for supporting in simulations by WUFI® Plus.

**References**

[1] Gigliarelli E, Calcerano F and Cessari L 2016 *EuroMed Conf 2016, Part I, LNCS* Vol **10058** eds Ioannides M et al. (Springer, Cham) pp 91–103
[2] Tronchin L and Fabbri K 2017 Energy and Microclimate Simulation in a Heritage Building: Further Studies on the Malatestiana Library *Energies* **10** 1621
[3] Lucchi E 2016 Multidisciplinary risk-based analysis for supporting the decision making process on conservation, energy efficiency, and human comfort in museum buildings *J. Cult. Herit.* **22** 1079-89.
[4] Roberti F, Oberegger UF, Lucchi E and Troi A 2017 Energy retrofit and conservation of a historic building using multi-objective optimization and an analytic hierarchy process *Energ. Buildings* **138** 1-10.
[5] Leissner J, Kilian R, Kotova L, Jacob D, Mikolajewicz U, Broström T, Ashley-Smith J, Schellen H L, Martens M, Van Schijndel J, Antretter F, Winkler M, Bertolin C, Camuffo D, Simeunovic G and Vyhlídal T 2015 Climate for culture: Assessing the impact of climate change on the future indoor climate in historic buildings using simulations *Herit. Sci.* **3** 1–15
[6] Camuffo D 2014 *Microclimate for Cultural Heritage- Conservation, Restoration, and Maintenance of Indoor and Outdoor Monuments* (Amsterdam: Elsevier) pp 557
[7] Holm A, Kuenzel H M and Sedlbauer K 2003 The hygrothermal behaviour of rooms : combining thermal building simulation and hygrothermal envelope calculation *Build. Simul.* 499–506
[8] Rode C and Woloszyn M 2007 Whole-building hygrothermal modeling in IEA Annex 41. Thermal Performance of Exterior Envelopes of Whole Buildings, *ASHRAE*, Atlanta, 2007, pp. 1–15
[9] Delgado JMPQ, Barreira E, Ramos NMM and de Freitas VP 2013 *Hygrothermal Numerical Simulation Tools Applied to Building Physics* (Springer-Verlag Berlin & Heidelberg) pp 66
[10] Künzel H M 1995 Simultaneous Heat and Moisture Transport in Building Components One- and two-dimensional calculation using simple parameters. Doctoral dissertation. (Stuttgart: University of Stuttgart, IRB-Verlag) pp 65
[11] Antretter F, Sauer F, Schöpfer T and Holm A 2011 Validation of a hygrothermal whole building simulation software. Fraunhofer-Institut für Bauphysik, Holzkirchen , Germany *Ashrae Stand.* 14–6
[12] Corcoran L, Duffy A and Rouholamin S 2013 *2nd Central European Symp for Building Physics,* eds Mahdavi A and B Martens (Vienna: University of Technology - Faculty of Architecture and Regional Planning) pp 305–12
[13] Schmidt S, Lindauer M and Hoppe M 2012 *Proc 5th Int Building Physics Conf (IBPC).* (Kyoto: Kyoto University) pp 1143–48
[14] Ozolins A, Jakovics A and Ratnieks A 2013 *Comsol Conf.* (Comsol Incorporated). 1–6
[15] Barclay M, Holcroft N and Shea A D 2014 Methods to determine whole building hygrothermal performance of hemp-lime buildings *Build. Environ.* **80** 204–12
[16] Bichlmair S, Raffler S and Kilian R 2015 The temperierung heating systems as a retrofitting tool for the preventive conservation of historic museums buildings and exhibits *Energy Build.* **95** 80–5
[17] Kurnitski J and Vuolle M 2000 Simultaneous Calculation of Heat, Moisture and Air Transport in an Modular Simulation Environment *Est. Acad. Publ.* 25–47
[18] Woloszyn M and Rode C 2008 Tools for performance simulation of heat, air and moisture conditions of whole buildings *Build. Simul.* **1** 5–24
[19] Napp M and Kalamees T 2015 Energy use and indoor climate of conservation heating, dehumidification and adaptive ventilation for the climate control of a mediaeval church in a cold climate *Energy Build.* **108** 61–71
[20] Napp M, Wessberg M, Kalamees T and Broström T 2016 Adaptive ventilation for climate control in a medieval church in cold climate *Int. J. Vent.* **15** 1–14
[21] Parish OO and Putnam TW 1977 Equations for the determination of humidity from dewpoint and psychrometric data. *Nasa Technical Note, NASA TN D-8401* 1–24